Available online at www.sciencedirect.com
SCIENCE DIRECT®

Journal of the European Ceramic Society 24 (2004) 1439–1448
www.elsevier.com/locate/jeurceramsoc

Novel high capacitance materials:- $BaTiO_3$:La and $CaCu_3Ti_4O_{12}$

Anthony R. West*, Timothy B. Adams, Finlay D. Morrison, Derek C. Sinclair

University of Sheffield, Department of Engineering Materials, Mappin Street, Sheffield S1 3JD, UK

Abstract

A review is given of the origins of high permittivity in two groups of materials, La-doped $BaTiO_3$ and a new barrier layer capacitor material, $CaCu_3Ti_4O_{12}$. Factors that influence permittivity include: dopant, doping mechanism, processing conditions and grain size. La-doped $BaTiO_3$ has high permittivity due to its ferroelectric nature at low temperatures and a novel doping mechanism: A-site substitution linked to the creation of B-site vacancies for charge compensation. Permittivities of 25,000 have been achieved, which can be increased further to ~36,000 by additional doping with Zr. The value of impedance spectroscopy to characterize materials that have heterogeneous electrical microstructures is illustrated with the example of $CaCu_3Ti_4O_{12}$; the high permittivity is not a bulk effect, as widely stated in the literature, but is a thin layer effect typical of a barrier layer capacitor. By attention to processing conditions to achieve large grain sizes, effective permittivities as high as 300,000 have been obtained.

Keywords: $BaTiO_3$ and titanates; Dielectric properties; Grain boundaries; Impedance spectroscopy

1. Introduction

Electroceramics can be grouped into two categories (Table 1), depending on whether, electrically, they are homogeneous or heterogeneous. As a consequence, the processing of electroceramic materials to optimise their properties is very different in the two cases. For electrically homogeneous materials such as most ionically conducting ceramics, or microwave dielectrics, it is usually desirable to have high-density ceramics in which the grain boundaries have no influence on the electrical properties. By contrast, materials such as varistors and barrier layer capacitors have properties that are controlled exclusively by the detailed chemistry and structure of interfacial regions at grain boundaries and grain surfaces. It may be less important to achieve high density ceramics in such cases; what is much more important is processing of the ceramics, often by a series of post-sintering heat treatments, so as to get the correct defect segregation, degree of oxidation/reduction, etc. at the grain boundaries and surfaces.

For the characterisation of electroceramics, it is useful to distinguish between the *ceramic microstructure* that is seen by direct observation using electron microscopy and the *electrical microstructure* that is determined indirectly by techniques such as impedance spectroscopy. In some cases, the ceramic and electrical microstructures match, but in many others they do not. Thus, just because grain boundaries are present in ceramics and seen easily by electron microscopy, it does not necessarily follow that they have any influence on the electrical microstructure. By contrast, grains, especially at grain surfaces, may show small variations in composition that are responsible for the characteristic properties of varistors and barrier layer capacitors and whereas it may be extremely difficult or impossible to detect such compositional variations by electron microscopy, these features are clearly present in the electrical microstructure and indeed, may dominate the overall electrical properties.

This review focuses on high permittivity dielectric materials, possible origins of high permittivity and some recent examples. High permittivity can be a bulk effect exhibited by ceramic grains such as in ferroelectric materials close to their Curie temperature at which significant ionic displacements, or polarisation, can occur in response to a small applied electric field. An excellent example is La-doped $BaTiO_3$; it has both an exceptionally high permittivity, >25,000 for selected compositions and temperatures,[1,2] and a novel doping mechanism to achieve high permittivity, consisting of A-site substitution (Ba by La) and B-site vacancies (Ti vacancies, to maintain charge neutrality).[3] An additional feature of La-doped $BaTiO_3$, however, is the need

* Corresponding author.
E-mail address: a.r.west@sheffield.ac.uk (A.R. West).

0955-2219/$ - see front matter © 2003 Elsevier Ltd. All rights reserved.
doi:10.1016/S0955-2219(03)00510-7

Table 1
Electrical microstructure of electroceramics

Electrically homogeneous	Electrically heterogeneous (grain boundary controlled)
Ionic conductors	Varistors
Mixed conductors	Barrier layer capacitors
High T_c superconductors	PTC thermistors
Microwave dielectrics	Gas sensors

to avoid oxygen loss during ceramic processing[4,5] since this can lead to other phenomena such as semiconductivity and positive temperature coefficient of resistance (PTCR) effects.[6]

Alternatively, high permittivity may be associated with sample geometry and, in particular, with thin layer effects associated with grain boundaries, surface layers or sample-electrode contacts.[7] In such cases, the equation that governs the overall capacitance, Eq. (1), contains three variables, the overall permittivity, ε' of the dielectric region, the cross-sectional area of this region, A and its thickness, l:

$$C = \varepsilon_o \varepsilon^1 A l^{-1} \quad (1)$$

where ε_o is the permittivity of free space, 8.854×10^{-14} Fcm^{-1}. Eq. (1) is implicit to the construction of high permittivity ceramic devices such as barrier layer capacitors (BLCs), in which thin insulating regions of material are connected by regions of ceramic that have high conductivity; BLCs are, therefore, classic examples of ceramics whose electrical microstructure is heterogeneous. Results are presented on a new material with possible BLC applications, $CaCu_3Ti_4O_{12}$; interestingly, this material has been claimed to show a 'giant dielectric effect'[8–10] whereas impedance spectroscopy (IS) results show that in fact, thin layer phenomena[11,12] are responsible for its high permittivity.

One of the experimental problems in probing the origins of high permittivity in a particular material concerns the need for experimental techniques that are able to distinguish bulk and grain boundary phenomena. Such a technique, which is finding increasing applications in the characterisation of electroceramics[13] and which was critical to establishing the electrical microstructure of $CaCu_3Ti_4O_{12}$, is impedance spectroscopy.

Impedance spectroscopy measures the response of materials to a small applied sinusoidal voltage. The technique covers a very wide range of frequencies up to and including the microwave region, although most instrumentation is limited to frequencies up to the megahertz range. Fig. 1 shows a schematic diagram of the phenomena that can be studied by IS, ranging from low frequency electrochemical processes to high frequency effects associated with dielectric relaxation and ion hopping between sites. The various phenomena are characterised by the difficulty and/or frequency of their occurrence; thus, lattice vibrations occur at infrared frequencies, approx 10^{12} Hz and there is no time interval between successive vibrations. Long range ionic conduction, by contrast, usually occurs by means of a process in which ions hop quickly from one site to another at lattice vibration frequencies, but then spend a considerable amount of time 'in residence' at a particular site before carrying out another hop. This overall hopping process, whether ionic or electronic (in electronic hopping semiconductors), may be measured as the sample resistance: a high resistance simply means that successive hops occur very infrequently! In addition, the process has an associated capacitance which effectively measures the lattice polarisation or response of the sample to the applied voltage. Such processes, involving a combination of lattice polarisation and ionic or electronic transport through different regions of a sample, including interfacial reactions, may be represented by combinations of parallel RC elements, (Fig. 2).

The fundamental link between such RC elements and the conductivity frequency spectrum, Fig. 1, concerns the magnitude of the relaxation frequency, ω, given by

$$\omega RC = \omega\tau = 1 \quad (2)$$

The various phenomena in the frequency spectrum (Fig. 1), are therefore separated according to the magnitude of their RC products or their relaxation times, τ and, therefore, according to the magnitudes of R and C associated with the different phenomena.

Impedance spectroscopy provides a powerful technique to investigate these effects, since the available frequency window on most instrumentation covers several decades of frequency, ω, typically 10^{-2} to 10^6 Hz, allowing relaxation times, τ in the range 10^2–10^{-6} s to be studied. Since many of the phenomena represented in Fig. 1 are temperature dependent, i.e. their resistance, R values, are temperature dependent, then it is possible to access different regions of the conductivity spectrum by varying temperature. In particular, the low frequency (large τ) effects may be accessed at higher temperatures at which reactions are speeded up sufficiently for their relaxation frequencies to be within the measuring range; conversely, phenomena such as local hops, which may occur very easily, can be accessed by reducing temperature, increasing the residence time between hops and therefore, increasing the resistance associated with such processes.

Impedance spectroscopy is particularly valuable for characterising electroceramics: first, the resistances of bulk and grain boundary regions in BLC materials are very different and also have different temperature dependencies; second, ferroelectric materials show classic Curie–Weiss dependence of their capacitance as a function of temperature,[14–16] whereas most materials, including dielectrics, have a capacitance that is essentially independent of temperature. By carrying out

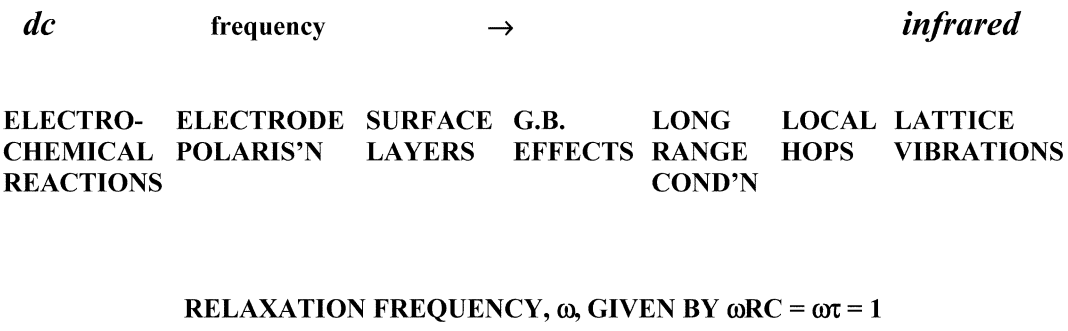

Fig. 1. The range of phenomena that can be studied in the ac conductivity spectrum over the entire range of frequencies from dc to infrared.

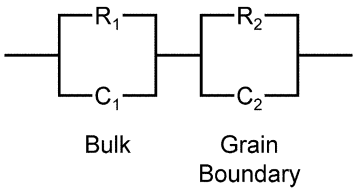

Fig. 2. An equivalent circuit consisting of combinations of RC elements that represent different regions of a heterogeneous electroceramic.

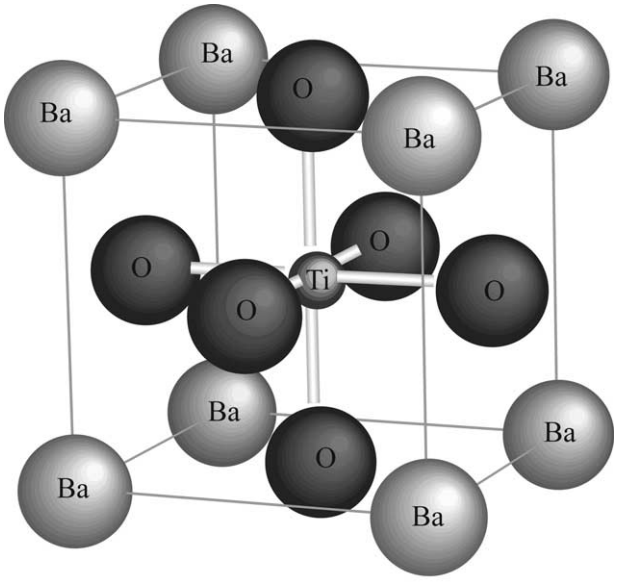

Fig. 3. Crystal structure of cubic $BaTiO_3$.

impedance measurements over a range of temperatures, therefore, it is usually possible to obtain a powerful insight into the electrical microstructure of ferroelectric materials and especially, to distinguish between ferroelectric and nonferroelectric components.[17]

2. $BaTiO_3$ and $BaTiO_3$:La

The classic high permittivity dielectric is, of course, $BaTiO_3$. In its cubic, high temperature form, stable above ca 130 °C, it has the simple perovskite structure (Fig. 3), containing TiO_6 octahedra. The reason why $BaTiO_3$ is such an interesting material and has a very high permittivity associated with the cubic to tetragonal phase transition that occurs on cooling at about 127 °C, is that the structure, containing Ba and Ti as the A and B cations, respectively, is at the limits of stability for the perovskite structure. This is because the Ba cations are rather large and effectively make the octahedral site for the Ti cations slightly too large giving a Ti–O bond distance of > 2 Å; Ti–O bond distances in TiO_6 octahedra are almost always in the range 1.94–1.96 Å and therefore, the Ti–O bond distance of > 2 Å is rather uncomfortable for the Ti^{4+} cation. Consequently, on cooling cubic $BaTiO_3$ through the phase transition to the tetragonal structure, a structural distortion occurs by means of which the *a* and *b* axes contract and the *c* axis elongates slightly; Ti cations displace off-centre from the TiO_6 octahedra giving a 5-coordinate arrangement with more reasonable Ti–O bond lengths and a much longer bond to a sixth oxygen, (Fig. 4).

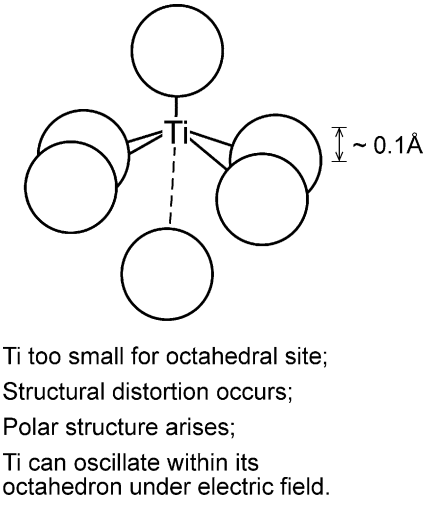

Fig. 4. Distorted TiO_6 octahedron in the perovskite structure of tetragonal $BaTiO_3$.

In tetragonal $BaTiO_3$ at room temperature, Ti cations in adjacent unit cells are displaced in the same direction,

giving domains in which the dipoles associated with the distorted, unsymmetric TiO_6 octahedra are aligned parallel. At room temperature, it is rather difficult to switch the orientation of the domains because this would require the titanium ions in adjacent TiO_6 octahedra to undergo a collective displacement towards one of the other six oxygens. This process is rather difficult and as a consequence the permittivity of $BaTiO_3$ at room temperature is reduced to around 10^3. This permittivity is, nevertheless, still high by comparison with that of common dielectric materials and is associated with displacement of Ti atoms at the edges and boundaries of the domains.

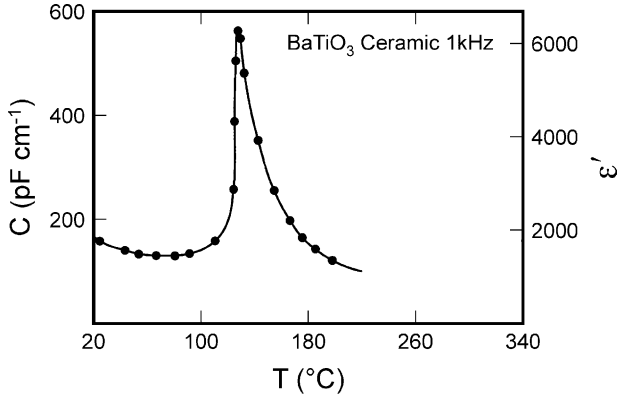

Fig. 5. Typical plot of permittivity against temperature for $BaTiO_3$

The temperature dependence of the permittivity of $BaTiO_3$ has the well-established classical form shown in Fig. 5, in which the permittivity passes through a maximum at the phase transition temperature, T_c, 127 °C. At this temperature, the long-range domain structure characteristic of the tetragonal phase disappears and hence the individual TiO_6 octahedra are able to respond essentially independently to an applied electric field; consequently, high permittivity results. At temperatures above T_c, in the paraelectric cubic region, although permanent domains no longer exist, nevertheless, the individual TiO_6 octahedra are probably distorted and the individual dipoles give rise to the classic Curie–Weiss response

$$\varepsilon' = C/(T - T_o) \quad (3)$$

where C is the Curie constant, T is temperature and T_o is the Curie Temperature.

Ionic displacement in solids is responsible for a wide range of phenomena and associated applications, as summarized in Fig. 6. With increasing degrees of ionic displacement, the associated properties change from low permittivity dielectrics to high permittivity dielectrics, to ferroelectrics and then to ionic conductors. For capacitor applications of ferroelectric materials, it is desired to increase the permittivity to as high a value as possible so that the miniaturisation of devices can be optimised. A summary of typical bulk permittivity values for a range of materials is given in Table 2. A well-studied

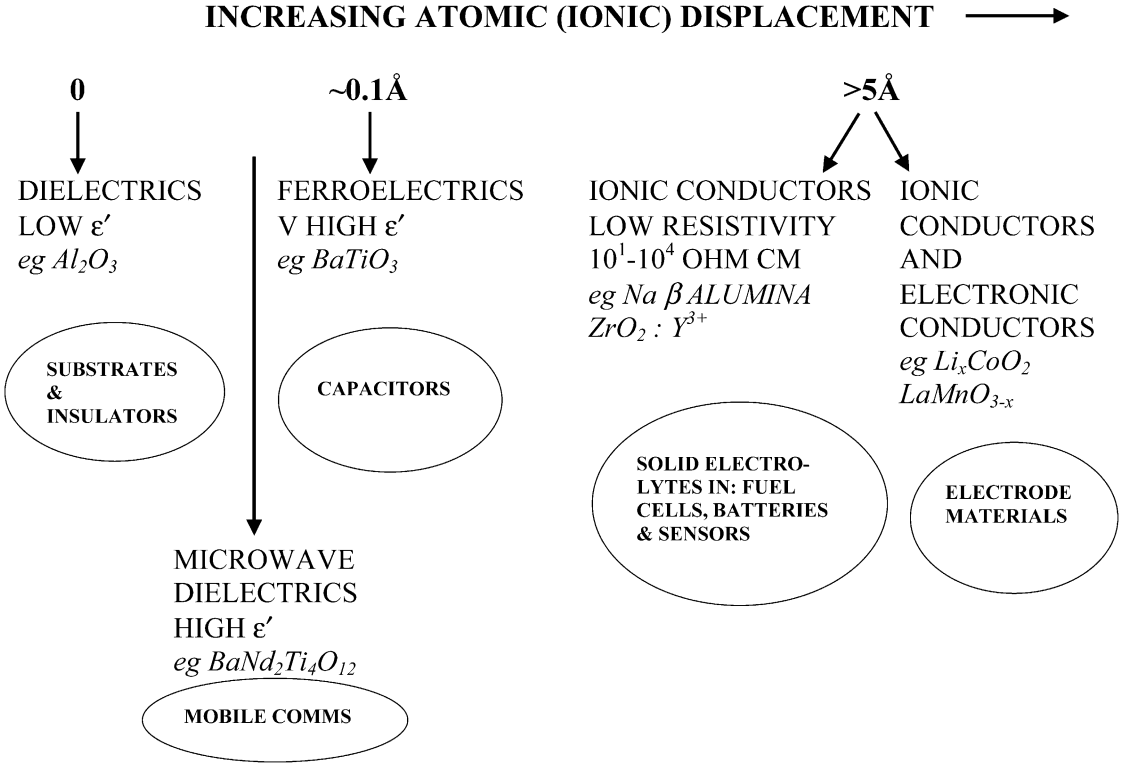

Fig. 6. Schematic diagram showing the range of properties and applications associated with ionic displacement in solids.

material with exceptionally high permittivity is the Pb–Mg–Nb perovskite, PMN;[7] in this case, the high permittivity is associated with the fact that the B-sites contain two cations of slightly different size, Mg and Nb. PMN is essentially a frustrated ferroelectric because the smaller Nb cations tend to displace off their octahedral sites giving rise to high permittivity, whereas the rather larger Mg cations are perfectly stable in the octahedral sites. Consequently, because the octahedral sites contain both cations, it is not possible for long-range domains to form. Given the toxicity of Pb, alternative materials to PMN are being sought for high permittivity applications.

For commercial applications of $BaTiO_3$, it is necessary to displace the ferroelectric Curie temperature, T_c, towards room temperature and also to broaden out the maximum in permittivity, ε'_{max}, so that the high permittivity can be obtained over a range of temperatures. This is usually done by double-doping in which some of the Ba is replaced by Ca and at the same time, some of the Ti is replaced by Zr. Such double-doped materials have been in use for many years as capacitor materials.

Table 2
Permittivity values of a range of dielectrics

Air	~1
Al_2O_3	~10
H_2O	~80
$BaTiO_3$ at T_c	~10,000
PMN ($PbMg_{1/3}Nb_{2/3}O_3$	~20,000

We have recently found, by a serendipitous discovery, that La-doped $BaTiO_3$, when processed so as to avoid oxygen loss, retains its insulating character, but also has T_c and ε'_{max} values that depend upon La content.[1–3] In studies of doping with aliovalent cations, i.e. of different charge to the ions that are being replaced, it is essential to have a clear understanding of the substitution mechanisms and in particular, the charge compensation mechanisms. There are two possible scenarios on aliovalent doping,[18] as summarized in Fig. 7 and for which the compensation mechanisms are either ionic or electronic. In the case of La-doped $BaTiO_3$, heated in air at temperatures below 1300 °C, or in O_2 at temperatures up to 1400 °C (these conditions being necessary to avoid small amounts of oxygen loss), then the compensation mechanism on substituting Ba by the higher valence La is to generate vacancies on the Ti sub-lattice.[3] The general formula of the solid solution that results is $Ba_{1-x}La_xTi_{1-x/4}O_3$: $0 < x < 0.2$. To determine the compensation mechanism, a phase diagram study of the ternary system $BaO–La_2O_3–TiO_2$ was required; the locus, or direction, of the solid solutions on the phase diagram found experimentally enabled various plausible compensation mechanisms to be considered, and rejected, since each of these would occur in different regions of the phase diagram, (Fig. 8). Further information on the link between phase diagrams and solid solution mechanisms is given in Ref. 3.

The variation in permittivity with x at ~0.1 MHz is shown in Fig. 9. The phase transition temperature decreases with increasing x and, for instance, occurs at about room temperature for $x = 0.05$. At the same time,

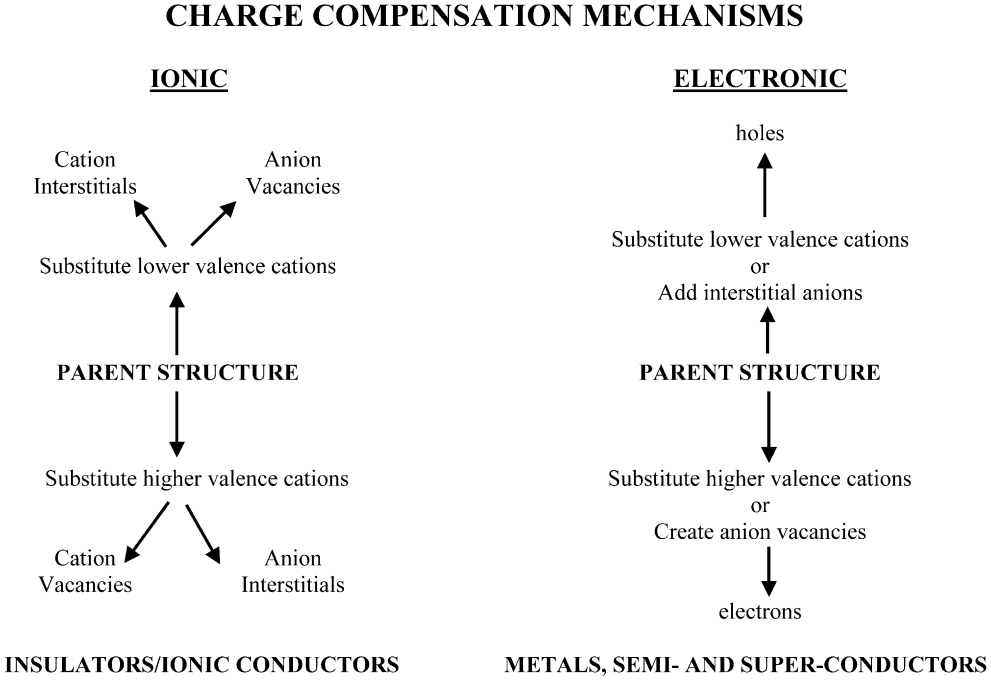

Fig. 7. Charge compensation mechanisms associated with aliovalent doping.[18]

the value of the permittivity at T_c increases and passes through a maximum of approximately 25,000 at $x = 0.06$ and -10 °C. With further increase in x, ε'_{max} decreases but also the peak becomes significantly broadened with temperature.

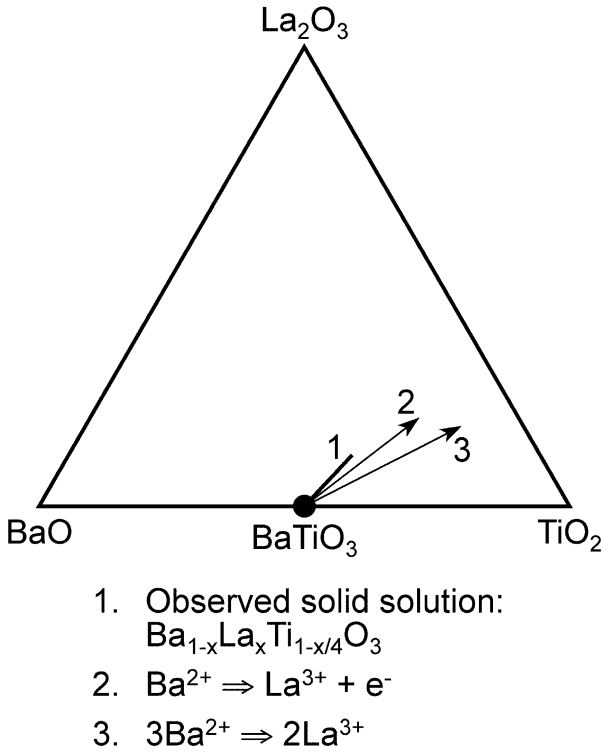

Fig. 8. Phase diagram BaO–La_2O_3–TiO_2 showing the location of La-doped $BaTiO_3$ solid solutions together with the directions of other plausible doping mechanisms.

Studies are presently underway to: (a) increase the permittivity still further; and (b) further broaden the permittivity maximum. Partial substitution of Zr onto the Ti site is particularly effective, as shown in Fig. 10. Commencing with composition $x = 0.05$, Zr is substituted for Ti according to the general formula $Ba_{0.95}La_{0.05}Ti_{0.9875-y}Zr_yO_3$. For $y = 0.05$, ε'_{max} reaches the exceptionally high value of 36,000 at a temperature of -30 °C.[19] Again, with increasing y, the peak broadens and at $y = 0.15$, the permittivity is frequency dependent and shows clear relaxor behaviour.

These results are particularly interesting scientifically since they give rise to a new mechanism of achieving very high permittivities, namely A-site substitution coupled to creation of B-site vacancies. In the same way that the domains in PMN are not able to form and grow because of the dissimilar Mg and Nb cations on the same set of B-sites, in La-doped $BaTiO_3$, the B-sites contain a mixture of Ti (and Zr) and vacancies which frustrates the desire of TiO_6 octahedra to form polar domains.

The behaviour described above of $BaTiO_3$:La refers to material that is fully oxidized. In partially-reduced materials, however, complications occur and additional properties are evident; in particular, partially-reduced $BaTiO_3$:La is semiconducting.[4,5] A long-standing puzzle in the literature concerns the origin of the semiconductivity and in particular, the switch-over from semiconducting to insulating behaviour which occurs

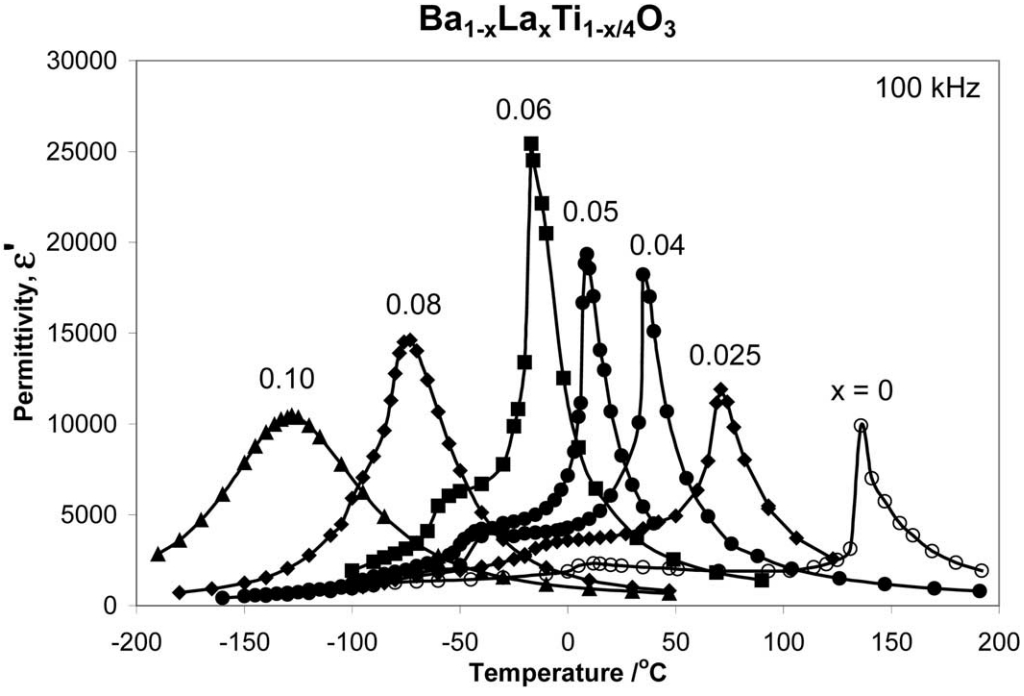

Fig. 9. Permittivity of La-doped $BaTiO_3$ as a function of La content.[2]

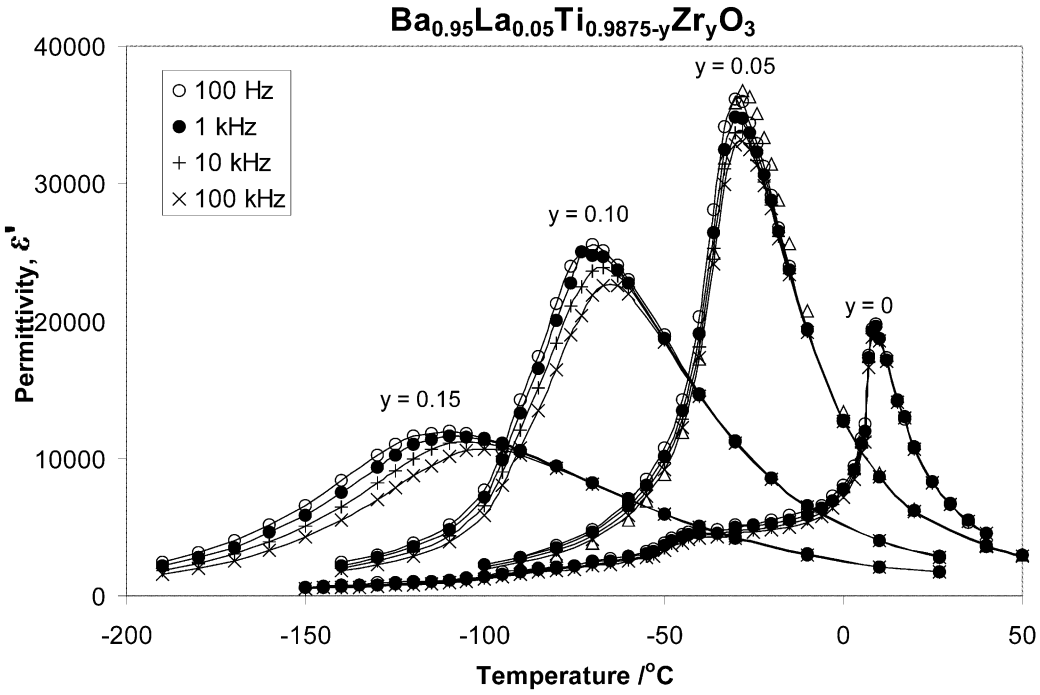

Fig. 10. Permittivity of $BaTiO_3$ double-doped with La and Zr as a function of Zr content.

abruptly at a certain, small, rare-earth content.[4] Much of the reason for the controversies and discrepancies in literature data arises because there are *two* mechanisms of achieving semiconductivity. One is so-called donor doping in which Ti^{3+} ions enter the lattice to compensate for introduction of La^{3+} ions, giving rise to the formula $Ba_{1-x}La_xTi^{4+}_{1-x}Ti^{3+}{}_xO_3$. This mechanism can certainly be introduced by synthesizing materials at high temperatures in reducing atmospheres. At this stage, it is not clear whether a limited amount of solid solution formation by this mechanism is possible under mild reducing conditions. The second mechanism of donor doping is via oxygen loss on heating at high temperatures $> \sim 1300$ °C. This may be represented by the simple equation:

$$O^{2-} \rightarrow 1/2\ O_2 + 2e^- \quad (4)$$

in which loss of oxygen causes the liberation of electrons which are retained in the crystal structure and are responsible for the semiconductivity.

The oxygen loss at high temperatures, Eq. (4), is rapidly reversible on cooling in air or oxygen and in particular, it is very easy to produce samples that are electrically heterogeneous and consist of reduced, semiconducting grain cores with oxidised, insulating grain boundaries and/or sample surfaces. As a consequence, the unusual composition-dependence of resistivity in samples of $BaTiO_3$:La heated in air at, e.g., 1400 °C, (Fig. 11), appears to arise from a combination of phenomena. The initial decrease in resistivity at low La contents may be due to either oxygen loss or direct doping with Ti^{3+}: it has not been fully established which mechanism is responsible and indeed both mechanisms may occur to differing extents, depending on the firing conditions. The increase in resistance at higher La contents does, however, appear to be a direct consequence of sample reoxidation on cooling rather than to a switch from electronic to

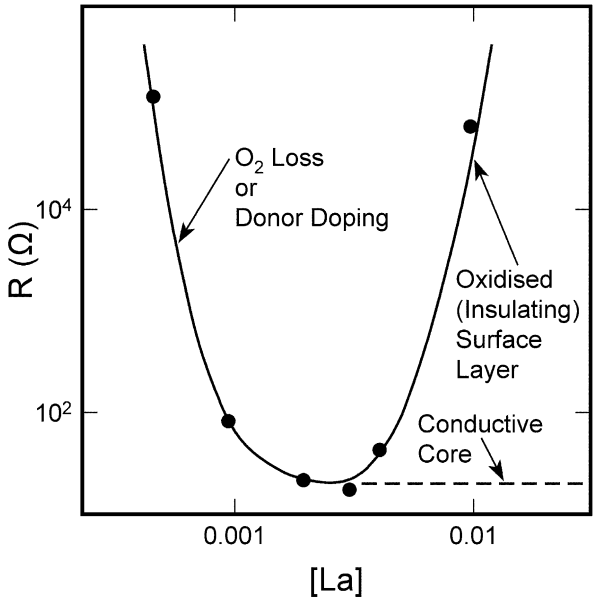

Fig. 11. Resistance of $BaTiO_3$:La ceramics as a function of La content for samples prepared and cooled in air.

ionic compensating mechanisms with increasing La content.

The electrical microstructure of partially reoxidized samples can be complex, as shown in Fig. 12, by impedance Z″ and modulus M″ spectroscopy; the combined spectra show at least three components: the low frequency, highly resistive component that dominates the Z″ spectrum and which is responsible for the overall insulating behaviour of the sample; and two higher frequency phenomena that are both semiconducting in nature and represent regions of the sample bulk.[5] The peak in the M″ spectrum at 10^4 Hz is attributed to grain surfaces since it has a capacitance of approximately 0.2 nF, whereas the highest frequency peak at $> 10^6$ Hz, with a capacitance <0.2 nF is attributed to the semiconducting grain cores.

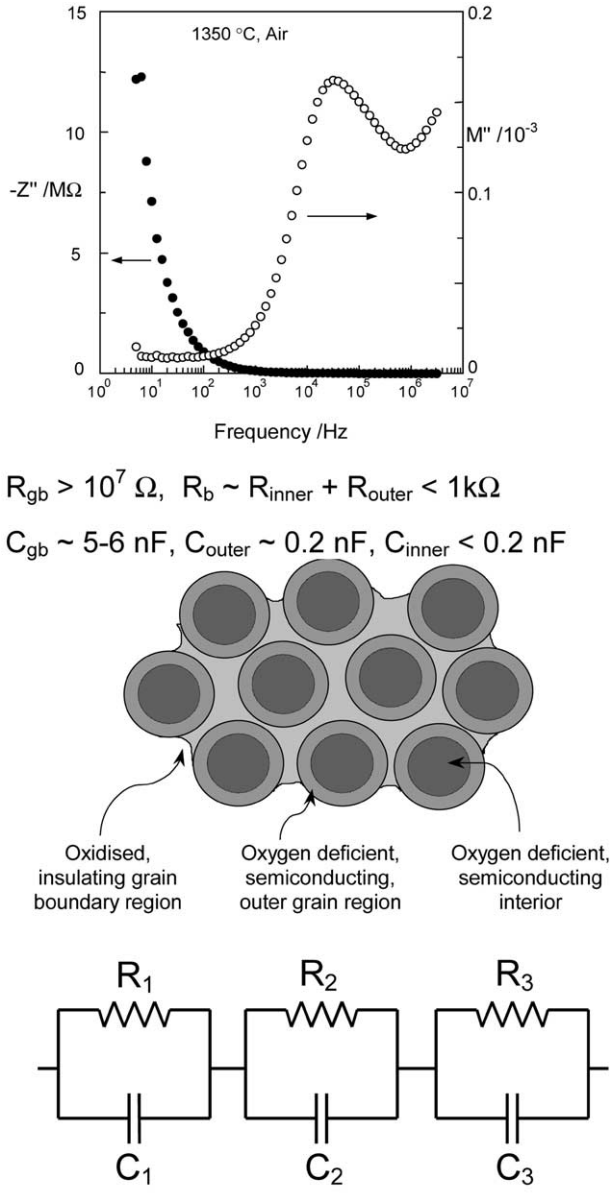

Fig. 12. Impedance Z″ and modulus M″ spectra of a partially reduced $BaTiO_3$:La ceramic showing conductive grain cores and insulating grain boundary regions.

2.1. $CaCu_3Ti_4O_{12}$

In the past two years, much interest in $CaCu_3Ti_4O_{12}$ has been generated with claims that it shows a giant dielectric response associated with some unknown feature of the bulk crystal structure.[8–10] $CaCu_3Ti_4O_{12}$ has an unusual perovskite-related crystal structure in which the TiO_6 octahedra are strongly tilted, giving rise to small, square planar coordinate sites for Cu in addition to the much larger A-sites for Ca. Several studies have shown that there is no evidence of any phase transition

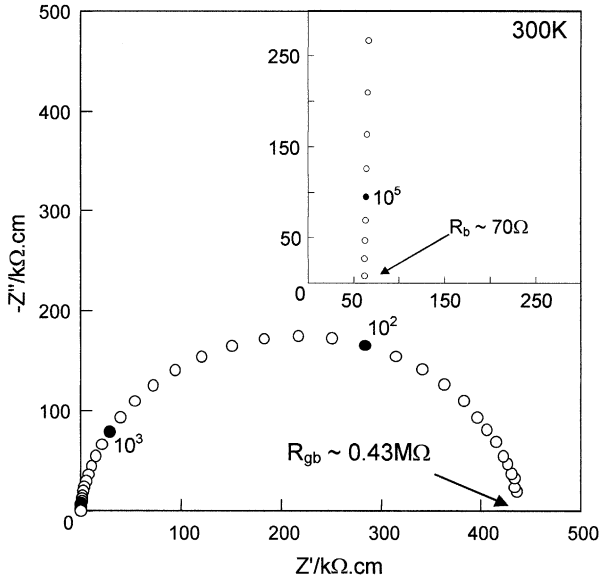

Fig. 13. Impedance data for $CaCu_3Ti_4O_{12}$ ceramic which can be interpreted as consisting of semiconducting grains with resistive grain boundaries.

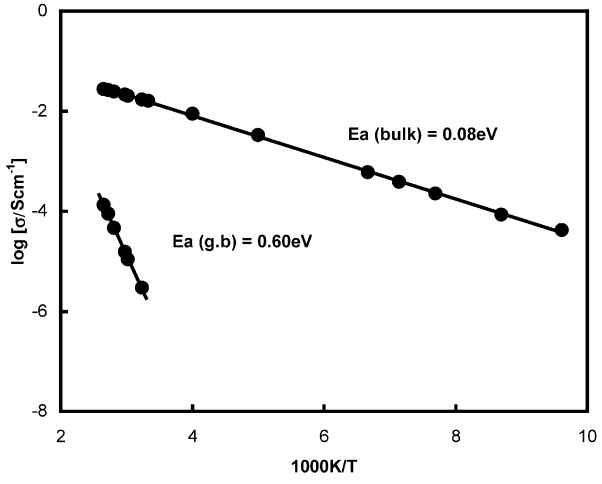

Fig. 14. Arrhenius plots of grain and grain boundary resistances extracted from impedance plots such as shown in Fig. 13.

in $CaCu_3Ti_4O_{12}$ nor any evidence of ferroelectric behaviour.[8,20] Impedance data on a ceramic sample sintered at 1100 °C and furnace cooled, are shown in Fig. 13. Two features are apparent; the data show a large arc with a total resistance of 0.43 MΩ but with a non-zero high frequency intercept and associated resistance of about 70 Ω. Both resistances are temperature dependent as shown in Fig. 14. Capacitance data (Fig. 15), show a high capacitance, low frequency plateau followed by, with increasing frequency, a dispersion region and a second high frequency, low permittivity plateau. These results are fully consistent with an equivalent circuit consisting of resistive grain boundaries and semiconducting grain cores and it is concluded that the so-called giant dielectric response is nothing more than a barrier layer capacitance effect.[11,12]

There are, nevertheless, intriguing questions remaining concerning $CaCu_3Ti_4O_{12}$. First, it is very surprising that the material can be fabricated as a barrier layer capacitor by a single step heat treatment in air involving sintering at 1100 °C followed by furnace-cooling over a period of 2–3 h; by contrast, to generate BLC phenomena in $BaTiO_3$-related materials requires very careful processing and several stages of heat treatment in different atmospheres.[7] Second, the origin of the bulk semiconductivity in $CaCu_3Ti_4O_{12}$ is not known; it could be an intrinsic mechanism or an extrinsic mechanism associated with departures from ideal stoichiometry. Third, the nature of the grain boundary regions is unknown; possibilities include: a variation in oxygen content compared with grain interiors; variation in cation composition between grain interiors and grain core; a secondary phase of different composition to the grains.

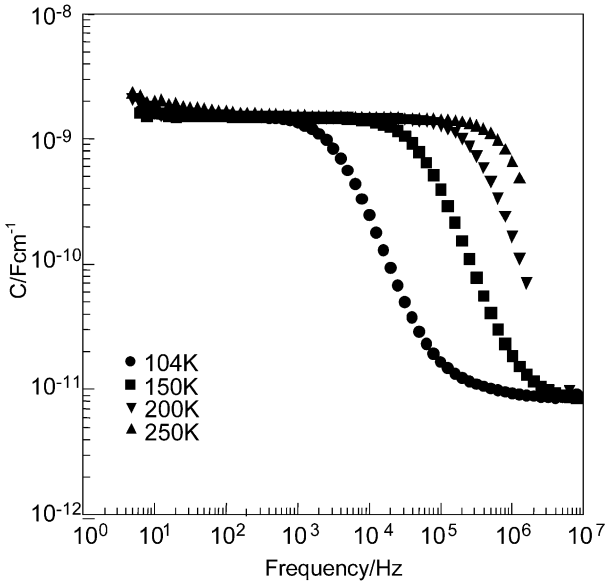

Fig. 15. Capacitance data as a function of frequency showing low and high frequency plateaux attributable to grain boundary and bulk capacitances, respectively.

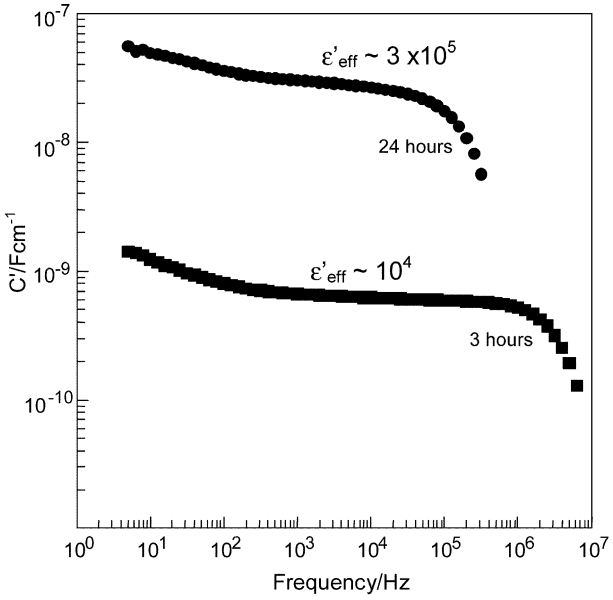

Fig. 16. Capacitance data as a function of grain size.

The effect of processing conditions on permittivity is illustrated in Fig. 16. On prolonged sintering at 1100 °C, grain growth occurs from an average of 30 microns after 3 h to about 300 microns after 24 h. The effective permittivity associated with the low frequency plateau increases from about 10,000 to about 300,000 as a consequence of the change in microstructure. This exceptionally high value offers the possibility of applications for $CaCu_3Ti_4O_{12}$ as a novel type of BLC.

Acknowledgements

We thank the EPSRC for financial support.

References

1. Morrison, F. D., Sinclair, D. C., Skakle, J. M. and West, A. R., Novel doping route to very high permittivity $BaTiO_3$ ceramics. *J. Am. Ceram. Soc.*, 1998, **81**, 1957–1960.
2. Morrison, F. D., Sinclair, D. C. and West, A. R., Electrical and structural characterisation of La-doped barium titanate ceramics. *J. Appl. Phys.*, 1999, **86**, 6355–6366.
3. Morrison, F. D., Coats, A. M., Sinclair, D. C. and West, A. R., Charge compensation mechanisms in La-doped $BaTiO_3$. *J. Electroceramics*, 2001, **6**, 219–232.
4. Morrison, F. D., Sinclair, D. C. and West, A. R., An alternative explanation for the origin of the resistivity anomaly in La-doped $BaTiO_3$. *J. Am. Ceram. Soc.*, 2001, **84**, 474–476.
5. Morrison, F. D., Sinclair, D. C. and West, A. R., Characterisation of lanthanum-doped barium titanate ceramics using impedance spectroscopy. *J. Am. Ceram. Soc.*, 2001, **84**, 531–538.
6. Morrison, F. D., Sinclair, D. C. and West, A. R., Doping mechanisms and electrical properties of La-doped $BaTiO_3$ ceramics. *Int. J. Inorg. Mater.*, 2001, **3**, 1205–1210.
7. Moulson, A. J. and Herbert, J. M., *Electroceramics: Materials, Properties and Applications*. Chapman and Hall, London, 1990.

8. Subramanian, M. A., Dong, L., Duan, N., Reisner, B. A. and Sleight, A. W., High dielectric constant in $ACu_3Ti_4O_{12}$ and $ACu_3Ti_3FeO_{12}$ phases. *J. Solid State Chem.*, 2000, **151**, 323–325.
9. Homes, C. C., Vogt, T., Shapiro, S. M., Wakimoto, S. and Ramirez, A. P., Optical response of high-dielectric-constant perovskite-related oxide. *Science*, 2001, **293**, 673–676.
10. Ramirez, A. P., Subramanian, M. A., Gardel, M., Blumberg, G., Li, D., Vogt, T. and Shapiro, S. M., Giant dielectric constant response in a copper-titanate. *Solid State Commun.*, 2000, **115**, 217–220.
11. Sinclair, D. C., Adams, T. B., Morrison, F. D. and West, A. R., $CaCu_3Ti_4O_{12}$: One-step internal barrier layer capacitor. *Appl. Phys. Lett.*, 2002, **80**, 2153–2155.
12. Adams, T. B., Sinclair, D. C. and West, A. R., Giant barrier layer capacitance effects in $CaCu_3Ti_4O_{12}$ ceramics. *Adv. Mater.*, 2002, **14**, 1321–1323.
13. Irvine, J. T. S., Sinclair, D. C. and West, A. R., Electroceramics: characterisation by impedance spectroscopy. *Adv. Mater.*, 1990, **2**, 132–138.
14. Sinclair, D. C. and West, A. R., Electrical properties of a $LiTaO_3$ single crystal. *Phys. Rev. B.*, 1988, **39**, 13486–13492.
15. Sinclair, D. C. and West, A. R., Impedance and modulus spectroscopy of semiconducting $BaTiO_3$ showing positive temperature coefficient of resistance. *J. Appl. Phys.*, 1989, **66**, 3850–3856.
16. Hirose, N. and West, A. R., Impedance spectroscopy of undoped $BaTiO_3$. *J. Am. Ceram. Soc.*, 1996, **79**, 1633–1641.
17. West, A. R., Sinclair, D. C. and Hirose, N., Characterisation of electrical materials, especially ferroelectrics by impedance spectroscopy. *J. Electroceramics*, 1997, **1**, 65–71.
18. West, A. R., Phase diagrams of inorganic materials: applications to complex solid-solution systems, site substitutions and stoichiometry-property correlations. *J. Mater. Chem.*, 1993, **3**, 433–440.
19. Morrison, F. D., Sinclair, D. C. and West, A. R., unpublished results.
20. Moussa, S. M. and Kennedy, B. J., Structural studies of the distorted perovskite $Ca_{0.25}Cu_{0.75}TiO_3$. *Mat. Res. Bull.*, 2001, **36**, 2525–2529.